Soft Matter

PAPER

View Article Online
View Journal

Cite this: DOI: 10.1039/c6sm01994c

Folding behavior and molecular mechanism of cross-linked biopolymer film in response to water†

Amrita Rath, Santhosh Mathesan and Pijush Ghosh*

Received 30th August 2016,
Accepted 15th October 2016

DOI: 10.1039/c6sm01994c

www.rsc.org/softmatter

Water responsive biopolymers are gaining enormous attention in the different areas of research and applications related to self-folding. In this work, we report that cross-linking is an efficient means of modifying a single layer biopolymer film for a controlled and predictable pathway of folding. The initiation of the folding of a film is caused by the diffusion of water molecules along the film thickness. However, this folding is observed to take place in an unpredictable and random fashion with a pristine biopolymer film and a nano-particle reinforced film. The mechanical properties and the diffusion characteristics of the film are strongly interrelated and affect the overall folding behavior. The underlying mechanism behind this relation is appropriately substantiated by an in depth molecular dynamic study. The detailed characterization of the folding shape and material behavior is performed applying suitable experimental techniques. The potential application of the controlled folding of the cross-linked film as a sensor and as a soft crane is demonstrated in this report.

Introduction

A smart biopolymer autonomously responds to stimuli, which can be in the form of water, pH, temperature, humidity, light, electric current, magnetic field and biological solvents.[1] One of the various ways of responding to these stimuli is the self-folding behavior. Self-folding metallic films and self-rolled tubes have been in use for a long time for various applications in transport, nano-optics, energy storage elements and for photovoltaic power applications.[2–5] However, they impose further difficulty due to their high rigidity, non-biodegradability, toxicity, compatibility issues and ineffectiveness in biomedical systems. Therefore, in the last decade, enormous attention has been paid to studying the stimuli responsive self-folding behavior of soft bio-polymeric materials.

Nature has provided enormous examples of smart materials, such as the opening of pine cones, the twisting of seed pods, the fast movement of Venus flytraps and many more in response to a particular stimulus. Observing closely these materials and understanding the underlying mechanism can be helpful when imitating them and creating smart synthetic materials. Reyssat *et al.* have studied pine cones as natural hygromorphs that respond to environmental humidity by changing their shape.[6] Li *et al.* have also used environmental humidity to show self-folding behaviors.[7] In a very recent report, Athas *et al.* have constructed a structure reminiscent of the Venus flytrap that transforms from an open to closed state upon exposure to an enzyme.[8] Janbaz *et al.* have designed a self-twisting DNA-inspired structure by using a bilayer made of shape memory polymers and hyperelastic polymers.[9] He *et al.* have developed a miniaturized self-folding device for improved drug transport, which folds depending on the change in pH level.[10] In another report, fabrication of free standing pH responsive hydrogel brushes has been demonstrated by Kang *et al.*[11] Breger *et al.* reported the development of photopatterned hydrogel bilayers composed of pNIPAm, AAc, HEMA and PEODA for actuating into 3D structures as a result of pH change.[12] The pH sensitive self-folding actuation has found application in the fields of drug delivery, non-evasive microsurgery, chemical sensors, filters, *etc.*[13–17] Simpson *et al.* designed a 3D system and were able to alter its structure and properties by controlling the temperature.[18,19] Stoychev *et al.* demonstrated the design of thermoresponsive NIPAM self-folding capsules for the controlled capture and release of cells in response to temperature signals.[20] In another report, Zhang *et al.* have shown the self-actuation of hybrid polymers driven in response to the day night rhythm of atmospheric humidity.[21] In another recent report, Zhang *et al.* fabricated moisture responsive self-folding films using cellulose

Nanomechanics and Nanomaterial Laboratory, Solid Mechanics Division, Department of Applied Mechanics & Soft Matter Center, Indian Institute of Technology Madras, Chennai-600 036, Tamil Nadu, India.
E-mail: pijush@iitm.ac.in

† Electronic supplementary information (ESI) available: Video V1_mechanical instability of three types of films; Video V2_chitosan as a soft crane; Video V3_chitosan film as a sensor; Video V4_chitosan film dipped fully inside water bath. See DOI: 10.1039/c6sm01994c

that also responds to temperature.[22] There are mentions of many others stimuli responsive self-folding behaviors of polymer systems being actuated by water, light, magnetic field, electric field and enzymes in excellent review papers.[23–25]

One of the challenges associated with the earlier reported works with metals and synthetic polymers is dealing with non-biodegradable materials.[23] Other challenges lie in demonstrating the self-folding behavior with 2D templates by using biopolymers.[26] These limitations paved the way for finding alternative soft biocompatible and biodegradable polymeric material for smart applications. The research in this particular field needs further advancement and is envisioned to play a pivotal role in future smart applications. However, one major setback with soft biopolymers is their extremely low mechanical properties which limit their further use in various disciplines, including self-folding applications. There are two commonly used approaches in the literature for enhancing mechanical properties, such as stiffness (E) and hardness (H) of a polymer matrix. The first approach is by reinforcement with a suitable nano-filler and the second by cross-linking the polymer with cross-linkers.

The nano-fillers employed in this work for improving the stiffness are biocompatible, biodegradable and similar in its mineral constituents of bone and having hydrophilic reactive sites. Hydroxyapatite (HAp) is applied as a representative hydrophilic nanofiller in nanocomposite film for studying hygro-responsive self-folding behavior. This is expected to show a similar behavior as compared to other nanofillers having hydrophilic reactive groups in terms of its interaction with water. Nanofillers in specific with hydrophilic groups have in prospect to affect the diffusion characteristics significantly, thus becomes a core interest of this folding behavior study. Further, the stiffness of the matrix is improved by cross-linking agent through 3D network structure formation. Glutaraldehyde (GA) is used in this case as a cross-linker and is anticipated to show a representative folding behavior with other cross-linked polymer systems. Desirable biorelated characteristics of GA in many biochemical applications when used in permissible limits makes it a potential cross-linker.[27] Chitosan, one of the most promising classes of biopolymers is examined in this particular work for studying self-folding behavior. Its ability to self-fold[28,29] in water classifies it as a smart biopolymer.

In this report, an *in situ* self-folding study of primarily three types of films (thickness $\sim$ 80 μm) is performed, which includes pristine chitosan (CS), hydroxyapatite chitosan (CSHAp) and cross-linked chitosan (CLCS) films. By applying the experimental methodology, the suitability of one particular type of film showing the predictable trajectory and controlled way of folding and unfolding is identified. This finding is significant as various applications demand a control over time as well as the rate of folding. Further, an innovative experimental methodology is followed by using existing goniometer set up for capturing the precise details of dynamic folding behavior that includes the displacement at various instances of time, rate of folding, change in the slope and total time of folding of CS and the modified CS films. The folding has a strong correlation with the way of interaction of polymer chains with the water molecules at the molecular level. The complex interplay of mechanical properties and diffusion characteristic affecting folding is understood by performing a molecular dynamic (MD) study. A systematic experimental observation and in-depth molecular mechanism study will play a pivotal role in controlled self-folding behavior, providing parameters for developing material models and its validation.

The driving forces behind self-folding can be many, and to list a few there is stress release, lattice mismatch, surface tension and swelling based self-folding.[30] Swelling based folding is of particular emphasis in this report. A differential change in volume due to non-homogeneous swelling allows the bottom surface of the film to stretch relatively more compared to the top surface of a single layer 2D film, thus resulting in differential strain along the thickness of the film. Then, the film unfolds and falls down when there is no differential strain in the top and bottom surface of the film. The folding of polymer films due to swelling can be broadly affected by two major factors: stiffness (mechanical property) of the polymer matrix and diffusion (physical property) of the polymer. These two properties are, however, strongly interconnected as diffusion phenomena significantly influence the mechanical properties and *vice versa*. Therefore, it is important to study the *in situ* self-folding behavior of the film in its pristine state as well as after modifying its stiffness by the two approaches mentioned above in order to make a suitable selection for specific applications.

All of the previously mentioned reports on bio-inspired models point toward a greater interest for sustainable biopolymers for self-folding applications, which is the focus of this study. In brief, this report primarily focuses on three main aspects of the folding behavior of CS biopolymer films. In the initial section the suitability of CS and modified CS films to undergo reversible and predictable pathways of folding and unfolding has been examined. Moreover, a comprehensive characterization of the folding behavior has been performed in terms of displacement at various instances of time, rate of folding, change in the slope and total time of folding. This section is followed by MD mechanism study of the interaction of the polymer film in the proximity of water. This study provides a deep insight into the corresponding mechanism responsible for the observed differences in the folding behavior of CS and modified CS film (CSHAp and CLCS). The last section discusses the experimental evidence of controlling the folding behavior by changing the degree of cross-linking, which is a requirement in various controlled self-folding applications as mentioned earlier. The potential of CLCS films in futuristic smart applications as a sensor and a soft crane is discussed and provided in Videos V2 and V3 (ESI†).

Results and discussion

Self-folding of chitosan films triggered by water contact

The water responsive behavior of a free standing chitosan film having a thickness $\sim$80 μm is demonstrated by studying its dynamic folding behavior at different instances of time.

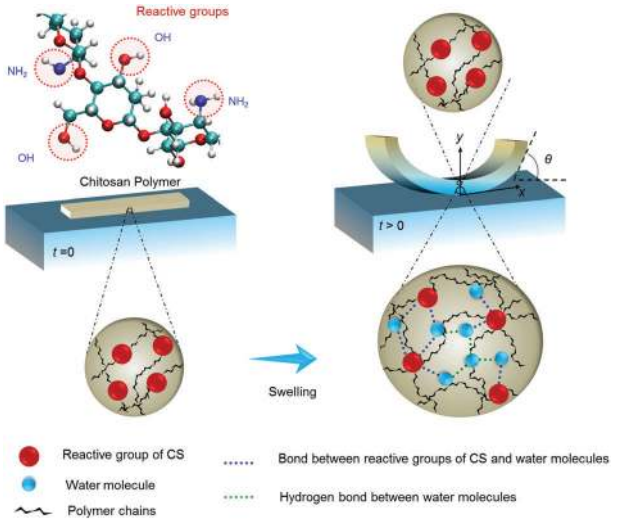

Fig. 1 Schematic representation of chitosan film folding due to differential swelling.

The self-folding behaviour of the film when only one side (bottom surface) is exposed to water is due to the existence of turgor pressure in the transverse direction to the plane of the film. This pressure gradient leads to differential strained surface layers having a higher stretched bottom surface (in water contact) compared to the top surface resulting in folding as shown schematically in Fig. 1. The figure shows that initially the film has a flat shape, followed by a gradual folding and unfolding in a predictable path every time. This folding behavior is reversible, *i.e.* it unfolds back to its original flat position and this behavior is repeatable a few times. This particular symmetrical pattern of folding from both sides has a strong dependence on its aspect ratio as reported earlier.[30] The folding phenomena take place gradually over a certain span of time with a corresponding change in the tip angle/slope of the film. By tracking this, the information about the rate of folding can also be obtained which carries significant information about the diffusion characteristics. This will be helpful in material modeling, designing and calibration of bio-films for a specified application. The experimental characterization of such folding behaviors is highly challenging and needs to be performed carefully to capture these behaviors. The procedure and set up applied to characterize this dynamic folding is explained in the Experimental section.

Furthermore, to demonstrate that the self-folding behaviour is not due to material inhomogeneity, experiments were performed by placing the film fully dipped inside the water bath and humidity chamber. As expected the film does not fold in either of these cases. The video of the film dipped along the vertical direction inside a water bath is Video V4 (ESI†).

Characterization of the folding shape of CS, CSHAp and CLCS films

Folding shape characterization of primarily three types of chitosan films, *i.e.* CS, CSHAp and CLCS films, are demonstrated in this section. Since this folding is symmetrical, the plot is shown taking the center point as the axis of folding.

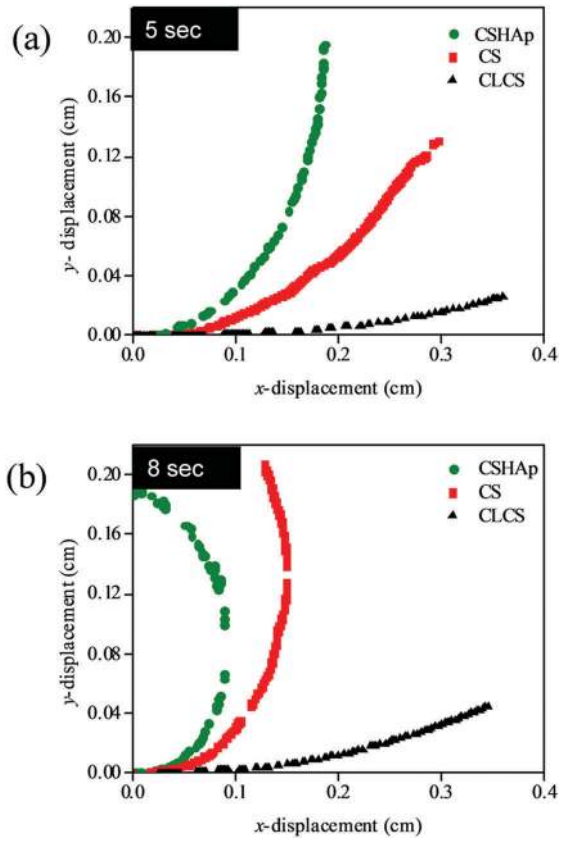

Fig. 2 A comparison plot showing x and y displacements during folding for CSHAp, CS and CLCS films at (a) 5 s and (b) 8 s.

The x and y displacement during the folding of the film for the above three cases is shown in Fig. 2a and b for 5 s and 8 s respectively. This plot provides the comparative study about the time taken for the complete folding and rate of folding of the above mentioned films. As observed from this figure, the time taken by the films to completely fold follows the order CSHAp $<$ CS $<$ CLCS. The total time taken for CSHAp, CS and CSCL film to completely fold is 8 s, 10 s and 26 s respectively, from the point of initiation of film folding. One of the most important observations from this study, which decides the workability of the film is the unfolding pattern of the film (shown in Video V1, ESI†). In our later sections, the unfolding feature of the film is shown to be useful in futuristic smart applications. Chitosan and CSHAp films in particular show a random or unpredictable unfolding pattern due to a loss of integrity and stability. Whereas a predictable path of unfolding is observed only in the case of CLCS films, which is similar to the path taken during the folding.

The structural stability in this context defines the ability of the film to perform folding and unfolding in a predictable path. It depends on various factors which can be broadly categorized into two, *i.e.* the mechanical properties (E and H) of the film and the diffusion characteristics of the film interacting with water. The stiffness of the material, however, degrades as a

Fig. 3 An optical microscope image showing experimental evidence of the improved stability of the CLCS film in terms of folding and unfolding compared to CS and CSHAp films.

function of time during folding since diffusion influences its mechanical properties. The loss in stiffness, in turn, affects its diffusion characteristics. The extent of influence in the properties is higher for CS and CSHAp films compared to CLCS films. This is reflected in the unfolding pattern of the film shown as experimental evidence in Fig. 3 (Video V1, ESI†). The molecular mechanism responsible for the reduction in mechanical properties is appropriately justified by the following MD mechanism study.

The interaction mechanism of water with a biopolymer, a hydrophilic nanoparticle biopolymer and a cross-linked biopolymer applying molecular dynamic studies

This section discusses the molecular interaction mechanism of a biopolymer (CS), a hydrophilic nanoparticle reinforced biopolymer (CSHAp) and a cross-linked biopolymer (CLCS) model system in the presence of water molecules. The MD study provides an insight into the difference in the folding behavior observed for the above mentioned film as a result of the diffusion characteristics and its influence on the stiffness of the polymer matrix for three different systems.

CS/water MD study

The primary functional groups of the biopolymer CS are the amine (NH_2) and hydroxyl (OH) groups. Within the CS system, amine groups and hydroxyl groups interact *via* hydrogen bond formation. However, in the presence of water molecules, the hydroxyl group of CS forms hydrogen bonds with water by remaining closer to the water molecules,[31] as shown in the Fig. 4a. These interactions are confirmed using radial distribution function (RDF) analysis. As a result of these interactions, some of the functional group sites in CS are occupied by the water molecules, thus, allowing an easy diffusion of the remaining water through the CS polymer chains. Therefore, the molecular interactions responsible for holding the chains together within the CS system become weaker. This leads to a reduction of the stiffness of the CS chains.

CS/HAp/water MD study

The model applied in the MD interaction study of CSHAp and water system is shown in Fig. 4b. The presence of HAp

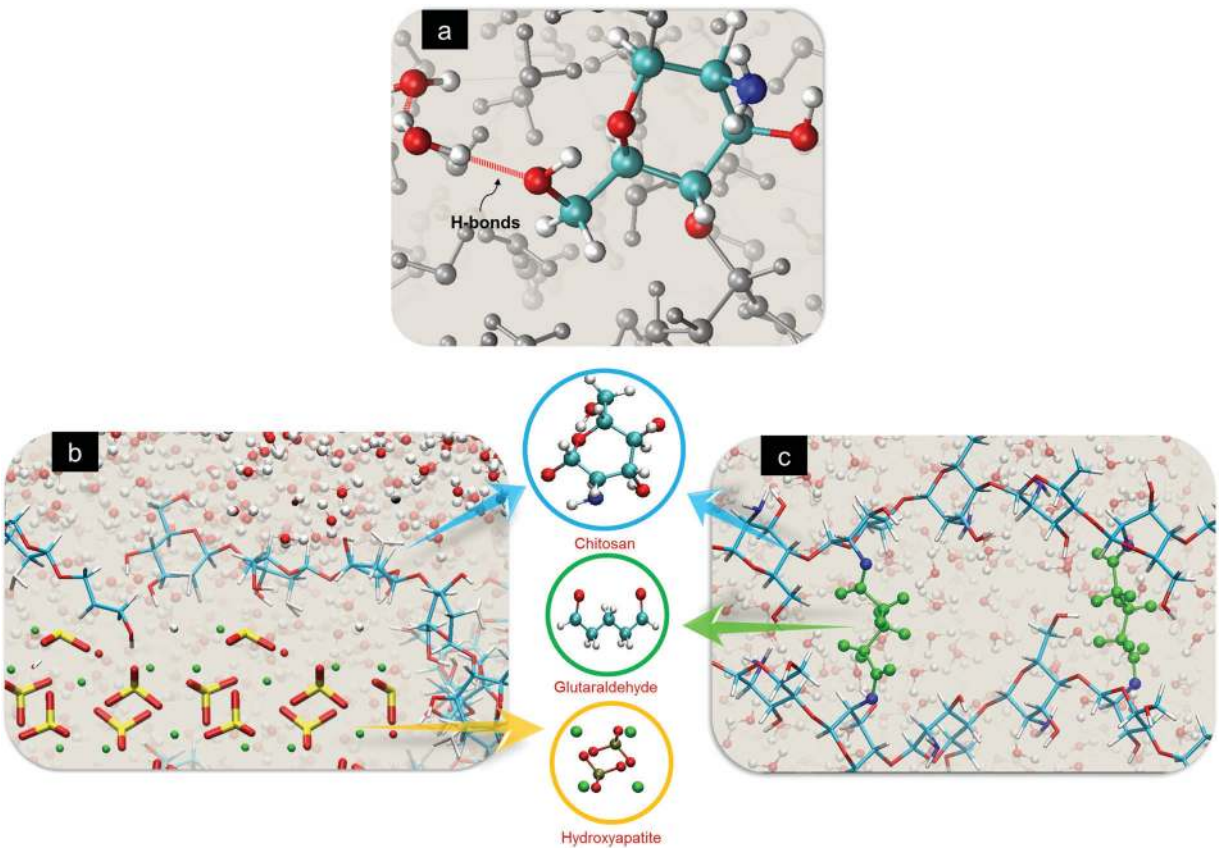

Fig. 4 (a) Hydrogen bond network within the CS water system, (b) molecular structure of the CSHAp system and (c) the CLCS system solvated with water molecules (hydrogen – white; oxygen – red; carbon – cyan; nitrogen – blue; colour coding for CPK representation, carbon – cyan; oxygen – red; hydrogen – white; calcium – green; phosphorous – tan gold).

nanoparticles improves the stiffness of the CS polymer matrix. One of the primary reasons is the restriction imposed by HAp towards changing or adoption of dihedral conformation of CS through reactive group interactions.[32–34] In the presence of water molecules, it is observed that the CS chains are no longer closer to the HAp surface, as they were during the initial stages of the simulation process. The water molecules diffuse through the chitosan chains to reach the HAp surfaces. The interactions between the OH and NH_2 groups of CS with the Ca^{2+} and PO_4^{3-} ions present in HAp are hindered due to the diffusion of water molecules towards the HAp surface.[33] Unavailability of the site of Ca^{2+}/PO_4^{3-} ions of HAp for CS results in the free movement of CS chains. Therefore, its dihedral conformations are not influenced by the HAp surface. Desorption of the CS chains from the HAp surface is captured at 0 ns, 1 ns, 5 ns and 8 ns, as shown in Fig. 5. The above mechanism is confirmed using a Radial Distribution Function (RDF) plot, which shows a reduced interaction between HAp and CS at longer times. The drop in interaction between HAp and CS in the presence of water medium leads to the loss of load transfer from the particle to the matrix. Thus, it reduces the stiffness necessary to maintain the structural integrity of the CS nanocomposites. Therefore, the nanocomposites tend to behave as a two phase material comprising of CS and HAp particles. This makes it

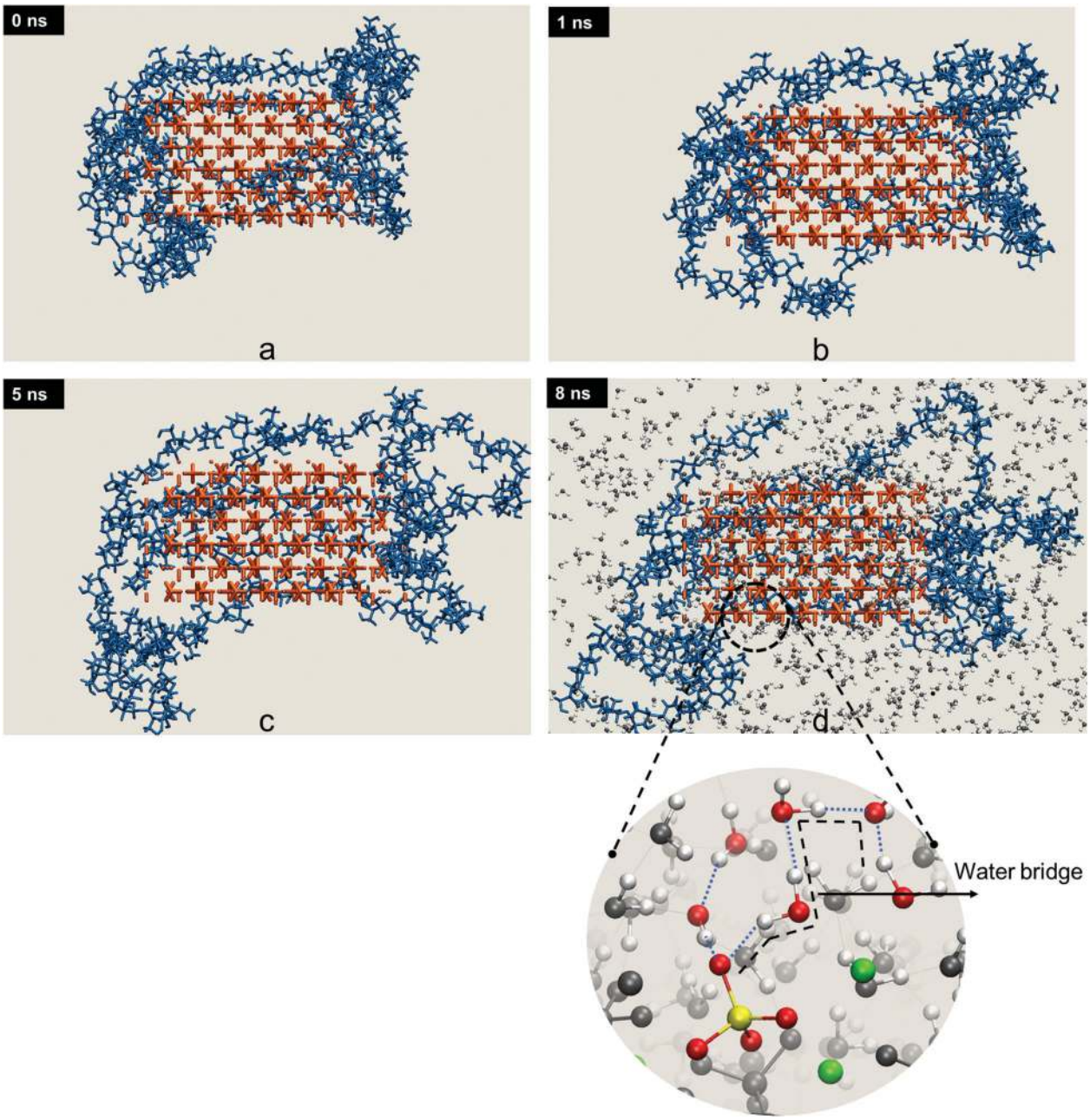

Fig. 5 Desorption of chitosan from the HAp surface after (a) 0 ns, (b) 1 ns, (c) 5 ns and (d) 8 ns of simulation (water molecules are removed from a, b and c for clarity). (Chitosan – licorice blue; hydroxyapatite – licorice orange; oxygen – red; phosphorous – yellow; calcium – green.)

unsuitable for self-folding applications, which is also confirmed from our experimental observations of the free movement of CS chains.

CS/CL/water MD study

It is experimentally verified that the cross-linked chitosan system performs a complete folding and unfolding process compared to a pristine and particle reinforced chitosan system. The cross-linked material systems in water medium possess adequate stiffness to perform self-folding phenomena. The variation of stiffness of the cross-linked CS system due to water molecules was understood by performing SMD (Steered Molecular Dynamics). SMD was performed on the pure CS system and the cross-linked CS system in the presence and absence of water molecules. The corresponding load displacement plot is obtained for the above mentioned systems as shown in Fig. 6a and the corresponding snapshots of the initial and final state from SMD as shown in Fig. 6b and c. During the initial stages of SMD, cross-linked-CS in the absence of water molecules tends to take a higher load compared to cross-linked CS in the presence of water molecules. This trend is because of the physical interactions that exist within the cross-linked CS system. In the presence of water molecules, these interactions are disturbed and thereby weaken the network structure. At the later stages of simulation, the three dimensional network structure formed due to GA molecules assists in maintaining the stiffness of the system.[33] The load carrying capability of cross-linked CS in the presence and absence of water molecules is almost the same at later stages of deformation. Also, it is noticed that the load carrying capability of pure CS completely reduces at later stages of deformation. Thus, making it unsuitable for the self-folding phenomenon. The above mechanism explains the suitability of the cross-linked system for self-folding phenomenon.

Slope variation of chitosan films during folding

The change in the shape of the film is accompanied by a change in the slope of the tip of the film, as shown in Fig. 7a–c. Measuring the slope is one of the primary means of quantifying

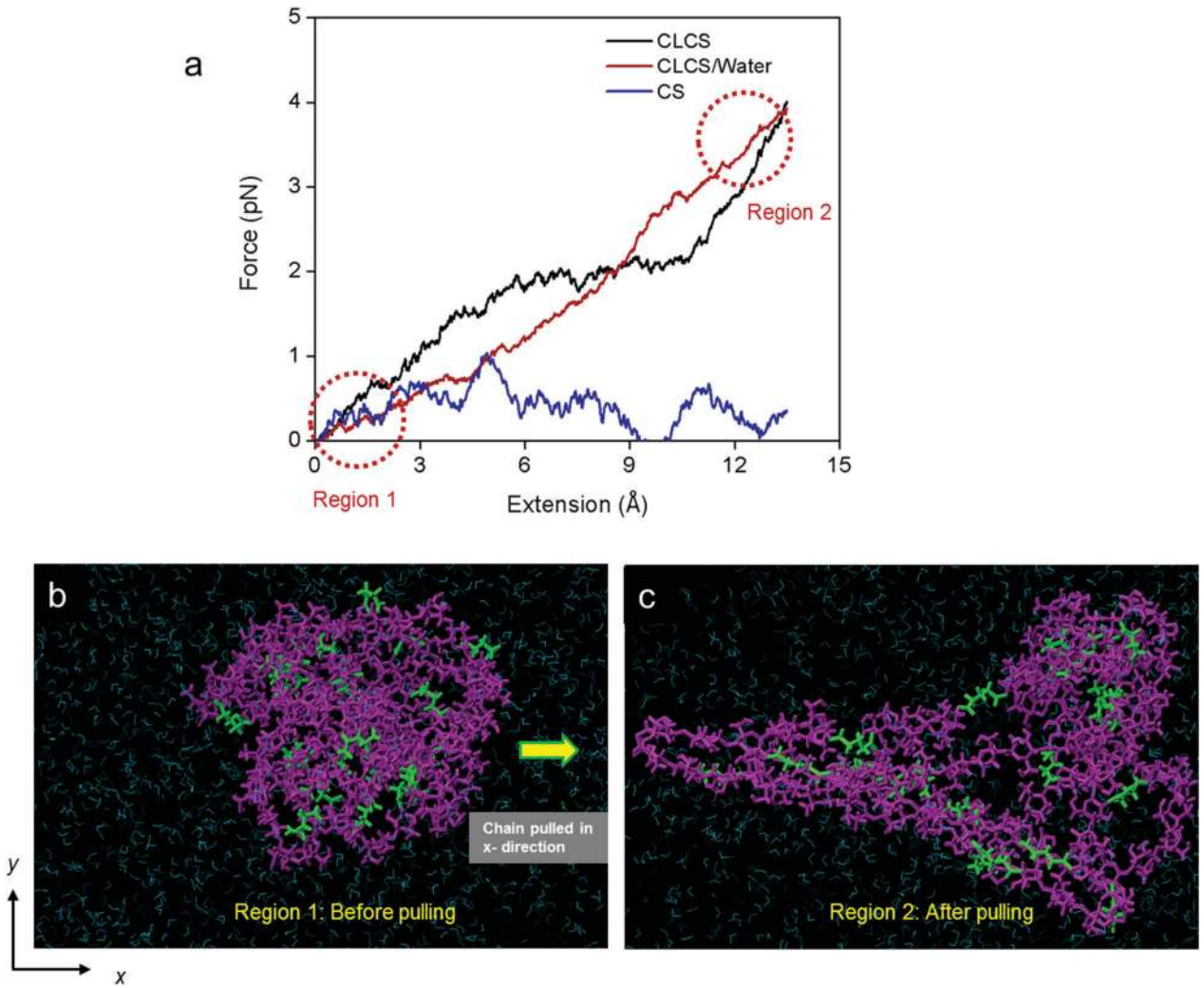

Fig. 6 (a) SMD force–extension profile for CS, CLCS and CLCS–water systems and their corresponding images of CLCS–water system (b) before pulling and (c) after pulling along *x*-direction. (Water molecule – line representation cyan; cross-linking agent – licorice green; chitosan – licorice purple.)

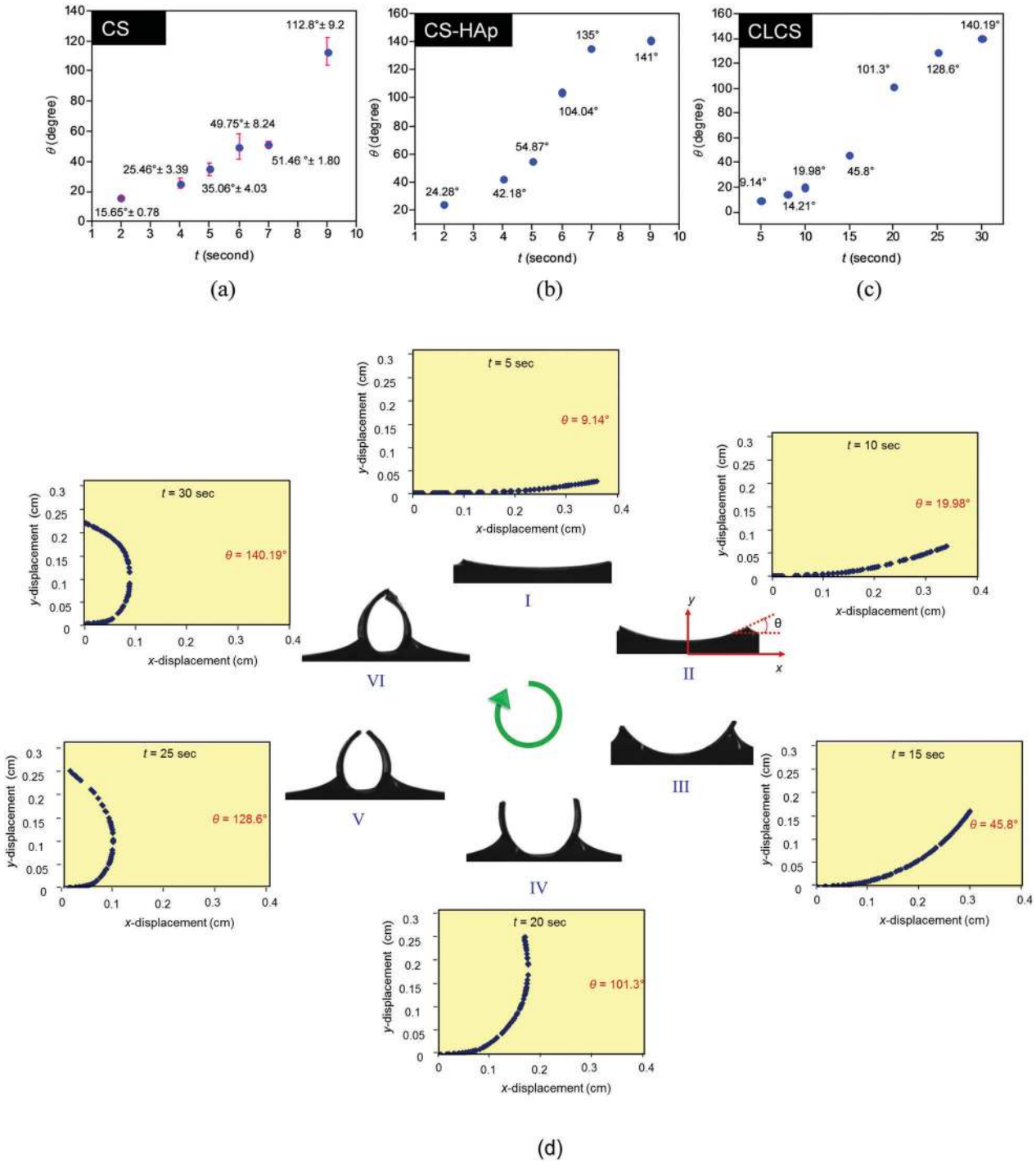

Fig. 7 The slope variation of the tip of the film during folding with the passage of time for the (a) CS, (b) CSHAp and (c) $CLCS0_{0.03}$ films and (d) the displacement profile of a representative $CLCS_{0.03}$ film folding placed in water at various instances of time.

the folding phenomena. All the experiments are repeated at least 3 times and the measurement of the average slope with a maximum standard deviation of approximately 9° is shown in the Fig. 7a. The change in slope of the CS and CSHAp films is shown for 10 s as the film completely folds within that time. However, the time taken for the same amount of folding for CLCS is comparatively higher.

In addition to this, one more relevant observation made from Fig. 7d is the rate of film folding. This is plotted only for the CLCS system since this is the actual system of interest compared to the other two systems. The rate of folding is observed to increase until 20 seconds, followed by a steep drop as shown in Fig. 8a. The drop in the curve is the result of the near saturation effect. This explains the reduction in the water

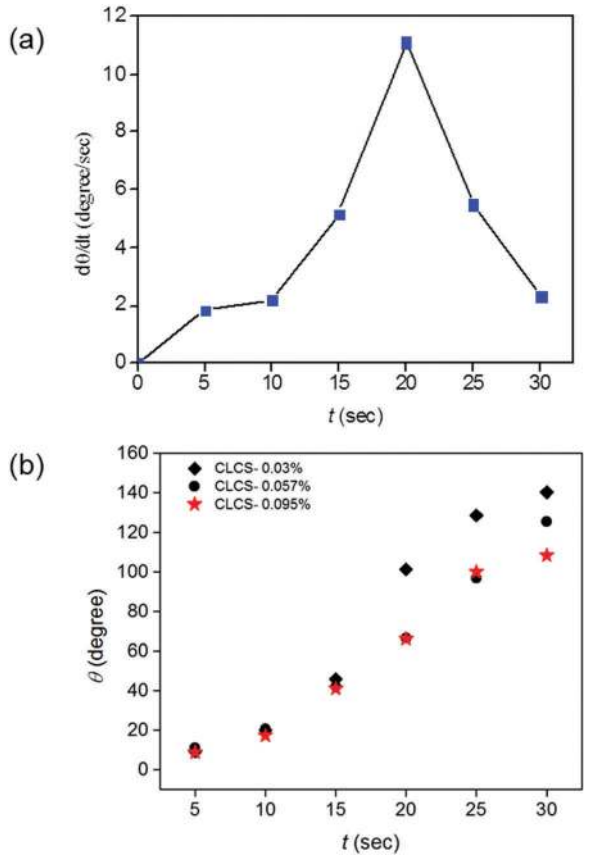

Fig. 8 (a) Rate of change of the slope of the $CLCS_{0.03}$ film with folding time and (b) the slope variation of the tip of the film with the passage of time for three different cross-linking contents.

diffusion due to the lesser availability of reactive groups present in the CLCS systems to form a bond with the water molecules. The reduction in the water diffusion is affected by the tension compression action during film folding as schematically shown in Fig. 9a. The folding causes tension and compression in the lower and upper half of the film respectively. The compression in the upper part could alter the diffusion path by changing the polymer chain orientation, chain entanglement, decrease in free volume, thus, affecting the rate of diffusion. This becomes a motivating factor for further the investigation of the mechanical properties on diffusion characteristics, which is the main focus of our immediate future work.

Effect of cross-linking (CL) content on folding

To study the effect of cross-linking on folding characteristics of the film, three different percentages of cross-linking (CL) agent, *i.e.* 0.03%, 0.057% and 0.095% are used in this study. Beyond 0.095% of CL agent, it is observed that the film cracks during the processing due to high brittleness. Moreover, it also imposed difficulty in cutting the film into the desired dimension due to brittle fracture of the film. Characterization of the folding shape along with the change in the angle is shown for a representative $CLCS_{0.03}$ film in Fig. 7d. The enhanced mechanical property leading to better workability and folding behavior of the film is observed due to addition of cross-linking agent to the pristine CS film. It is also noticed that the slope of the film reduces with increasing content of cross-linking agent at a particular time frame as shown in Fig. 8b. The reduction in slope is related to increase in total folding time. With $CLCS_{0.03}$, the total folding time is measured $\sim$26 s, which increases to $\sim$32 s for $CLCS_{0.057}$ and $\sim$35 s for $CLCS_{0.095}$. As mentioned earlier, for $CLCS_0$ (pure CS film), this folding time is 10 s. In a similar way, by changing the cross-linking content, the total time can be varied over a time frame of approximately 10–35 s, which gives an estimation of the total folding time that can be achieved in this case. This observation is critical for designing a film for a particular situation demanding necessary control over folding time. Interestingly, for a very high content of CL ($CLCS_{0.095\%}$), the film folds, but does not connect the opposite ends completely unlike the previous cases of folding. This is dependent on the aspect ratio of the film used for folding. For a lower CL, content the film will fold as well as connect opposites ends for different aspect ratio film. For a very high CL content, the film will not fold completely irrespective of different aspect ratio. However, for different aspect ratio, the critical CL content (minimum CL content at which the film will not connect opposite ends) will vary. For the aspect ratio followed in this manuscript, the critical CL content is observed at $CLCS_{0.095}$. Moreover, the folding and connecting the opposite ends of the film is an interesting phenomenon which can be engineered to be used as a sensor for measuring either humidity level, identifying pH of particular solvent, detecting biological molecule or any other entity of desired interest in a solvent. Therefore, for these applications a very high degree of cross-linking content is not desirable.

Nanomechanical characterization of chitosan films

The depth sensing nanomechanical characterization is performed on CS, CSHAp and CLCS films to determine the material's Young's modulus (E) and hardness (H). Owing to the small dimension of the film in the actual field of use and higher spatial resolution, quasi-static nanoindentation is a more convenient technique compared to bulk mechanical characterization. The indentation is carried out on both dry as well as wet films (fully saturated with water). The method followed for dry film is explained in detail in our previous work and the E and H values obtained for the CS and CSHAp films are 1.49 $\pm$ 0.07 GPa and 0.11 $\pm$ 0.01 GPa, and 2.43 $\pm$ 0.47 GPa and 0.13 $\pm$ 0.02 GPa, respectively.[32] The E and H values for the cross-linked films are performed in the current work and calculated as 3.08 $\pm$ 0.15 GPa and 0.21 $\pm$ 0.005 GPa, respectively. The mechanical properties of the CLCS films are observed to be higher compared to both CS and CSHAp. As the CLCS film is the actual system of our interest, its mechanical properties at fully saturated conditions (wet state) are measured applying nanoindentation by using a fluid cell tip. The E and H values are 38.3 $\pm$ 8 MPa and 6.6 $\pm$ 2.8 MPa, respectively.

Equilibrium swelling behaviour of chitosan films

The equilibrium swelling ratios of the CS, CSHAp and CLCS films that affects the overall folding behavior are determined by using gravimetric measurements. Specimens are immersed in fresh DI water and the change in weight of the swollen film till

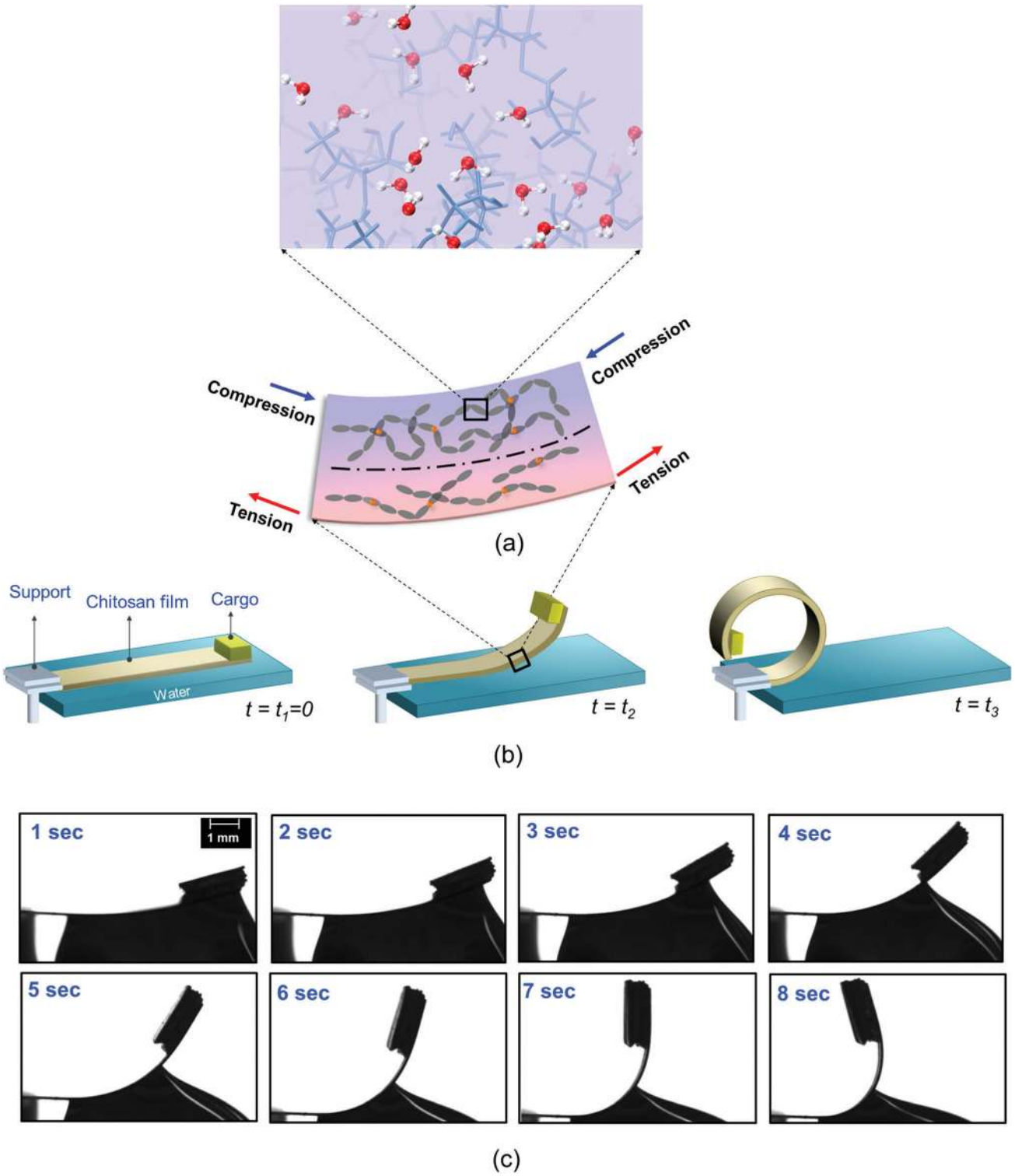

Fig. 9 (a) Schematic representation of the zoomed view of tension and compression region in the film during folding, (b) schematic representation of the lifting of cargo by the CLCS film during folding and (c) the snapshot of cargo lifting at various time instances by the CLCS film.

it reaches the equilibrium swelling is measured. The equilibrium swelling ratio of CS, CSHAP and CLCS at a time interval of 60 min is determined to be 10171.15% ± 277.35%, 4371.62% ± 332.72% and 161.54% ± 1.37%, respectively. The high degree of swelling of the CS and CSHAp films compared to the CLCS films affects the mechanical properties of the film. During the swelling process, the chains present in the polymer matrix tend to move away from each other due to the diffusion of water. This behaviour of chain movements is relatively high for CS and CSHAp compared to CLCS, thus reducing its mechanical

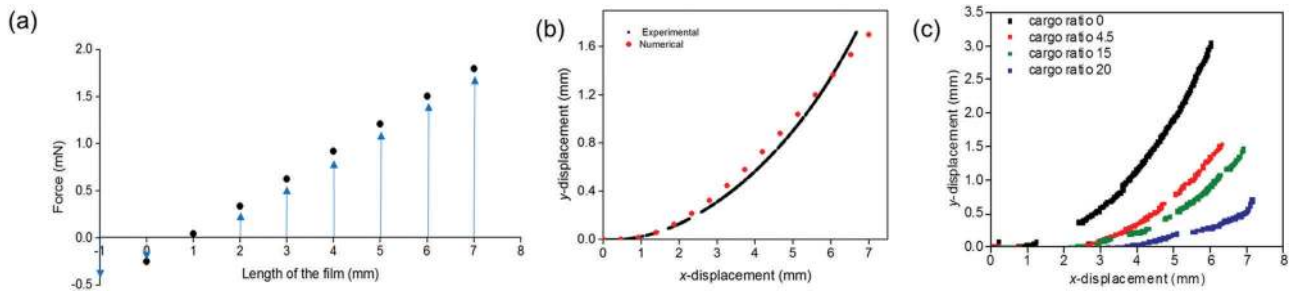

Fig. 10 (a) The variation of force functions with the x-displacement for cantilever film folding at 1 s, (b) a plot showing the displacement curve fitting of experimental and numerical data at 1 s and (c) x and y coordinates of the CLCS film during lifting of various cargo ratios at t = 3 s.

properties significantly. This is reflected in the folding pattern of the film as shown in Fig. 3. The molecular mechanism of the higher swelling ratio of CS and CSHAp compared to the CLCS film is explained in detail in the previous section.

Load carrying capacity of chitosan film

The symmetrical folding behavior of the film can be used as a possible soft crane for lifting a cargo. A CLCS film is found to be suitable for this purpose as the other chitosan films (pure CS and CSHAp) lose their mechanical stability upon being exposed to water and are not capable of lifting any load. In order to accomplish the lifting of a cargo, a CLCS film is fixed at one end to impose a cantilever boundary condition, while the other end is left free as shown schematically in Fig. 9b. The film is loaded with various weight ratios of cargo : film, *i.e.* 0, 4.5, 15, 20 and 25 in order to determine its maximum load carrying capacity. The snapshot of the film lifting cargo for a weight ratio of 4.5 is shown in Fig. 9c. The maximum load carrying capacity is determined for the film and demonstrated in Video V2 (ESI†). It was also observed that with all these loads, the total folding time remains nearly same, which is ~15 s. However, in the initial phase of the lifting, a delay in the response time is observed, which is shown at 3 s from the start of folding as shown in Fig. 10c. The force function and bending stress developed during the folding of the film without cargo is determined here. The deflection of the film at t = 1 s is analyzed in ABAQUS 6.10.1 assuming the theory of a linear elastic beam. The chitosan film is modeled as a 2D line element with the cantilever boundary condition. The material properties, Young's modulus (E) and Poisson's ratio (ν), are 3.08 ± 0.15 GPa and 0.3, respectively. The force function acting on the film is analytically determined from the experimental curve. The displacement y as a function of x is determined from the experimental curve. By substituting EI in the force equation

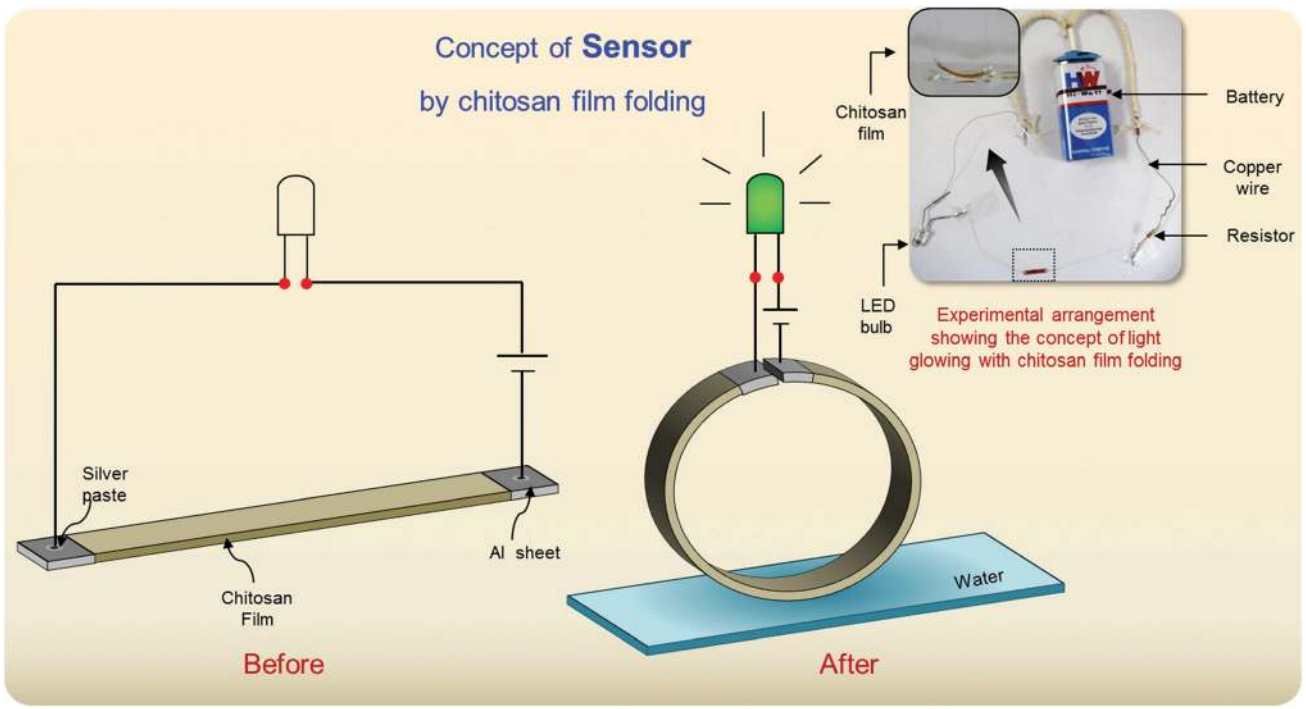

Fig. 11 A schematic representation of the concept of light glowing by using the CS film folding phenomena.

given by $F(x) = EI(dy^4/dx^4)$, the transverse force function acting on the film is obtained as:

$$F(x) = 0.00029207x - 0.00024953.$$

The variation of force as a function of x-displacement is shown in Fig. 10a. The obtained force function is given as an input to the solver. The displacement obtained is in good agreement with the experimental values, as shown in Fig. 10b. The bending stress in this case is found to be 16 MPa. This result is shown for the cantilever film after 1 s. However, this theory fails for deflections at a higher time frame due to the introduction of non-linearity in the problem. This has to be studied applying advanced theories of large strain, which is a standalone study by itself. This study only provides an idea of the type of force function and the stresses developed during the initial phase of folding.

Application of chitosan film folding as a sensor

A preliminary concept of applying the above principle of symmetrical folding as a sensor is shown in Video V3 (ESI†) as a proof of the concept. This video shows the glowing of an LED light when the film end points get connected during the folding process. The chitosan film showing folding behavior can be designed as a possible humidity sensor, as shown schematically in Fig. 11. This kind of folding behavior is demonstrated by using only the CLCS film as discussed in earlier sections. The folding time and the measured quantity need to be appropriately calibrated prior to use.

Conclusion

The objective of this particular study is to determine the suitability of chitosan films to undergo folding and unfolding in response to water. For that, chitosan was modified by a cross-linking agent and reinforced with nanoparticles. The cross-linked chitosan film is identified to be the most desirable for the purpose of controlled and predictable pathways of folding and unfolding. A comprehensive characterization of the folding behavior in terms of its displacement, total time, rate and slope of folding are determined for all types of films studied. This experimental characterization will be helpful in the development of material model as well as its validation. The cross-linked chitosan film also has the potential to have control over the total time of folding, which can be altered between approximately 15–35 s by varying the concentration of the cross-linking content. The mechanism responsible for identifying the suitability of a particular film for folding purposes is understood by performing a molecular dynamics study. The complex interplay of stiffness of the polymer and interaction of the polymer in the presence of water decides the suitability of the film to undergo folding. Chitosan and nanoparticle reinforced chitosan are observed to lose their stiffness due to interaction with water molecules, thus making it unsuitable for folding. Whereas, a three dimensional network structure formation for a cross-linked system assists in maintaining the stiffness even in the presence of water. This is reflected in the controlled way of folding for cross-linked chitosan film compared to other film types. As a proof of concept, the cross-linked chitosan film is shown to be applied as a sensor and as a possible soft crane in the attached Videos V2 and V3 (ESI†).

Experimental section

Material

Chitosan powder (degree of deacetylation >90%, viscosity (100–200) cps, medium molecular weight), were supplied from SRL Pvt. Ltd (India). Hydroxyapatite nanopowder, <200 nm size (BET), glutaraldehyde (25% aqueous solution), and acetic acid, >99.7% were purchased from Sigma Aldrich (India, Bangalore). Petri dish of size $\phi 35$, 15 mm thickness was used for pouring chitosan solution to make film.

Fabrication of chitosan films

Uncross-linked chitosan films. Chitosan solution (1.5% w/v) was prepared by dissolving 150 mg of CS powder in 10 mL of acetic acid (1% v/v). The solution was stirred by keeping over a hot plate magnetic stirrer at $\sim$45 °C for 2 hours forming a homogenous solution. Low speed stirring was applied to avoid formation of bubbles inside the CS solution. The homogeneous solution was poured into a clean Petri dish and kept in oven for $\sim$15 hours to dry. A CS film of $\sim$80 μm thickness was formed and stored in desiccators for further use.

Chitosan–hydroxyapatite films. To the above prepared homogenous pure CS solution, HAp powders were added slowly. The entire solution was maintained at $\sim$45 °C for 48 hours for homogeneous mixing of HAp powders with CS solution. After uniform mixing, the solution takes pale yellow color unlike pure CS film. The CS–HAp solution was poured into a clean Petri dish and kept inside oven to dry.

Cross-linked chitosan films. Cross-linked CS films were prepared by adding glutaraldehyde as a cross-linking agent to the above prepared pure CS film. Cross-linking amounts of 0.037%, 0.057% and 0.095% [glutaraldehyde (200 μL, 300 μL and 500 μL respectively) to the CS ratio (525 mg)] were added slowly to the already stirring CS solution. The cross-linked CS solution was immediately poured into the Petri dish before it became too viscous. The solution was kept in an oven for 12 hours for the solvent to evaporate, leaving behind a film of $\sim$80 μm thickness.

Film preparation for folding

The films obtained from the solvent casting method are cut into small rectangular shapes of 0.15 cm × 0.7 cm dimensions. The residual stress induced in the film during vacuum heating is removed by placing the cut samples between two glass slides and heating for 2–3 hours at 60 °C. The other purpose for keeping it between glass slides is to ensure the flatness of the film for further tests. The prepared film is kept on top of the water droplet and captured using an optical microscope placed perpendicular to the film. The goniometer setup is used for characterizing the folding behavior of all types of films as

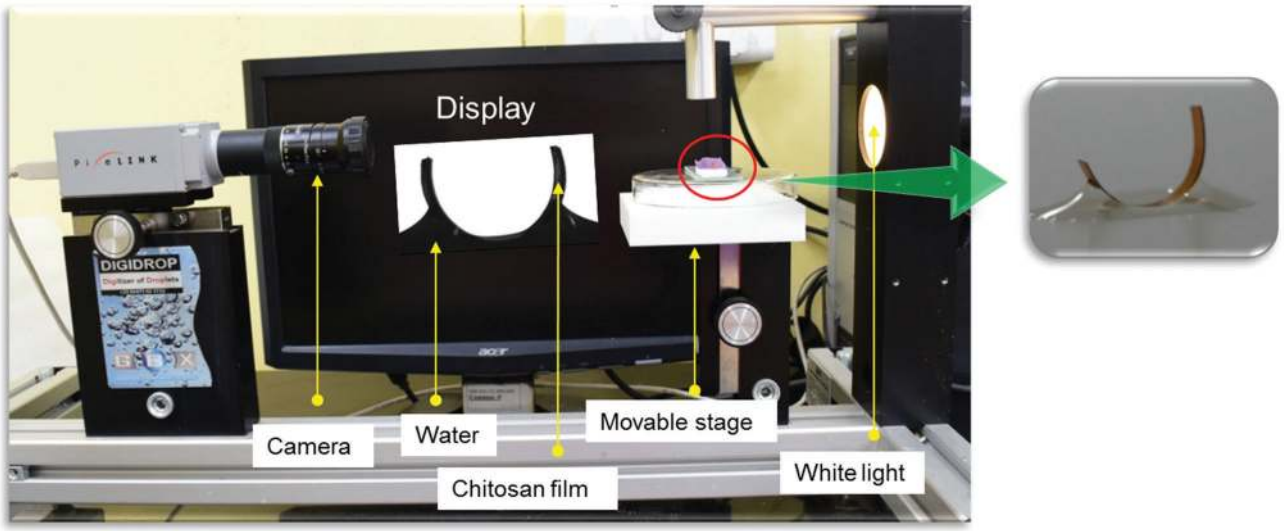

Fig. 12 An experimental set up for characterizing the folding behavior of the chitosan films.

shown in Fig. 12. All the experiments are repeated at least 3 times.

Molecular dynamics simulation details

In this particular study three types of systems, *i.e.* CS/water, CS/HAp/water and CS/CL/water are modeled and analyzed applying molecular dynamics simulation using LAMMPS.[35] All the systems were parameterized using the CHARMM forcefield.[36,37] For all the above three models, two CS chains with a chain length of 50 monomer units were used. The CS chains are minimized and equilibrated to build an amorphous system. In order to understand the behavior of CS chains in the presence of particles, CS chains are allowed to interact with HAp nanoparticles as shown in Fig. 5a. The cross-linked CS system is obtained by cross-linking the CS chains using glutaraldehyde (GA) as shown in Fig. 5b. Glutaraldehyde is a bifunctional molecule which reacts with the nitrogen of CS to form imine bonds. The cross-linked CS structure is preequilibrated using the *NVT* ensemble. The pre-equilibrated CS, HAp reinforced CS and cross-linked CS systems are solvated using modified TIP3P water model molecules. The temperature of all the systems is gradually increased from 1 K to 300 K with a step of 30 K. Each step of temperature rise is followed by equilibration for 50 ps. The CS/water and CS/CL/water systems are subjected to MD simulation for 1 ns, whereas, the CS/HAp/water system is subjected to it for 8 ns.

Notes and references

1 D. H. Gracias, *Curr. Opin. Chem. Eng.*, 2013, **2**, 112–119.
2 E. W. Jager, O. Inganäs and I. Lundström, *Science*, 2000, **288**, 2335–2338.
3 J. S. Randhawa, T. G. Leong, N. Bassik, B. R. Benson, M. T. Jochmans and D. H. Gracias, *J. Am. Chem. Soc.*, 2008, **130**, 17238–17239.
4 M. Jamal, N. Bassik, J.-H. Cho, C. L. Randall and D. H. Gracias, *Biomaterials*, 2010, **31**, 1683–1690.
5 S. Schwaiger, M. Bröll, A. Krohn, A. Stemmann, C. Heyn, Y. Stark, D. Stickler, D. Heitmann and S. Mendach, *Phys. Rev. Lett.*, 2009, **102**, 20–23.
6 E. Reyssat and L. Mahadevan, *J. R. Soc., Interface*, 2009, 951–957.
7 X. Li and M. J. Serpe, *Adv. Funct. Mater.*, 2014, **24**, 4119–4126.
8 J. C. Athas, C. P. Nguyen, B. C. Zarket, A. Gargava, Z. Nie and S. R. Raghavan, *ACS Appl. Mater. Interfaces*, 2016, **8**, 19066–19074.
9 S. Janbaz, R. Hedayati and A. A. Zadpoor, *Mater. Horiz.*, 2016, DOI: 10.1039/c6mh00195e.
10 H. He, J. Guan and J. L. Lee, *J. Controlled Release*, 2006, **110**, 339–346.
11 C. Kang, S. N. Ramakrishna, A. Nelson, C. V. M. Cremmel, H. V. Stein, N. D. Spencer, L. Isa and E. M. Benetti, *Nanoscale*, 2015, **7**, 13017–13025.
12 J. C. Breger, C. Yoon, R. Xiao, H. R. Kwag, M. O. Wang, J. P. Fisher, T. D. Nguyen and D. H. Gracias, *ACS Appl. Mater. Interfaces*, 2015, **7**, 3398–3405.
13 V. Luchnikov, O. Sydorenko and M. Stamm, *Adv. Mater.*, 2005, **17**, 1177–1182.
14 K. Kumar, V. Luchnikov, B. Nandan, V. Senkovskyy and M. Stamm, *Eur. Polym. J.*, 2008, **44**, 4115–4121.
15 T. S. Shim, S. H. Kim, C. J. Heo, H. C. Jeon and S. M. Yang, *Angew. Chem., Int. Ed.*, 2012, **51**, 1420–1423.
16 N. Bassik, B. T. Abebe, K. E. Laflin and D. H. Gracias, *Polymer*, 2010, **51**, 6093–6098.
17 S. Singamaneni, M. E. McConney and V. V. Tsukruk, *ACS Nano*, 2010, **4**, 2327–2337.
18 B. Simpson, G. Nunnery, R. Tannenbaum and K. Kalaitzidou, *J. Mater. Chem.*, 2010, **20**, 3496.
19 V. Stroganov, S. Zakharchenko, E. Sperling, A. K. Meyer, O. G. Schmidt and L. Ionov, *Adv. Funct. Mater.*, 2014, **24**, 4357–4363.

20 G. Stoychev, N. Puretskiy and L. Ionov, *Soft Matter*, 2011, **7**, 3277.
21 L. Zhang, H. Liang, J. Jacob and P. Naumov, *Nat. Commun.*, 2015, **6**, 7429.
22 K. Zhang, A. Geissler, M. Standhardt, S. Mehlhase, M. Gallei, L. Chen and C. Marie Thiele, *Sci. Rep.*, 2015, **5**, 11011.
23 L. Ionov, *Soft Matter*, 2011, **7**, 6786.
24 L. Ionov, *Adv. Funct. Mater.*, 2013, **23**, 4555–4570.
25 A. Agrawal, T. Yun, S. L. Pesek, W. G. Chapman and R. Verduzco, *Soft Matter*, 2014, **10**, 1411–1415.
26 C. L. Randall, E. Gultepe and D. H. Gracias, *Trends Biotechnol.*, 2012, **30**, 138–146.
27 On the Toxicology and Carcinogenesis Studies of Dipropylene Glycol in F344/N Rats and B6C3F 1 Mice (Drinking Water Studies) National Toxicology Program. 2004, No. 25265.
28 J. Guan, H. He, D. J. Hansford and L. J. Lee, *J. Phys. Chem. B*, 2005, **109**, 23134–23137.
29 M.-C. Chen, H.-W. Tsai, Y. Chang, W.-Y. Lai, F.-L. Mi, C.-T. Liu, H.-S. Wong and H.-W. Sung, *Biomacromolecules*, 2007, **8**, 2774–2780.
30 G. Stoychev, S. Zakharchenko, S. Turcaud, J. W. C. Dunlop and L. Ionov, *ACS Nano*, 2012, **6**, 3925–3934.
31 E. F. Franca, L. C. G. Freitas and R. D. Lins, *Biopolymers*, 2011, **95**, 448–460.
32 A. Rath, S. Mathesan and P. Ghosh, *J. Mech. Behav. Biomed. Mater.*, 2015, **55**, 42–52.
33 S. Mathesan, A. Rath and P. Ghosh, *Mater. Sci. Eng., C*, 2016, **59**, 157–167.
34 E.-S. M. El-Sayed, A. Omar, M. Ibrahim and W. I. Abdel-Fattah, *J. Comput. Theor. Nanosci.*, 2009, **6**, 1663–1669.
35 S. Plimpton, *J. Comput. Phys.*, 1995, **117**, 1–42.
36 O. Guvench, E. R. Hatcher, R. M. Venable, R. W. Pastor and A. D. J. MacKerell, *J. Chem. Theory Comput.*, 2010, **5**, 2353–2370.
37 O. Guvench, S. S. Mallajosyula, E. P. Raman, E. Hatcher, K. Vanommeslaeghe, T. J. Foster, F. W. Jamison and A. D. Mackerell, *J. Chem. Theory Comput.*, 2011, 3162–3180.